Contents lists available at ScienceDirect

Ocean Engineering

journal homepage: www.elsevier.com/locate/oceaneng

Highlights

Nonlinear bending behavior of a multilayer copper conductor in a dynamic power cable

Ocean Engineering xxx (xxxx) xxx

Haitao Hu, Jun Yan*, Svein Sævik, Naiquan Ye, Qingzhen Lu, Yufeng Bu

- The bending hysteresis behavior of a multilayer helically wound copper conductor in a dynamic power cable is studied.
- The bending hysteresis curve of a copper conductor is obtained by prototype tests.
- A 3D finite element model is established to study the bending hysteretic behavior of the copper conductor.
- The influence of friction coefficients between copper wires and between copper wire and outer sheath layer on the bending hysteretic behavior is discussed.
- The influence of the radial extrusion pressure on the bending hysteretic behavior is discussed.

Contents lists available at ScienceDirect

Ocean Engineering

journal homepage: www.elsevier.com/locate/oceaneng

Nonlinear bending behavior of a multilayer copper conductor in a dynamic power cable

Haitao Hu [a,b], Jun Yan [a,b,*], Svein Sævik [c], Naiquan Ye [d], Qingzhen Lu [b,e], Yufeng Bu [a]

[a] State Key Laboratory of Structural Analysis for Industrial Equipment, Department of Engineering Mechanics, Dalian University of Technology, No. 2 Linggong Road, Dalian, 116024, China
[b] Ningbo Research Institute of Dalian University of Technology, Ningbo 315016, China
[c] Department of Marine Technology, Norwegian University of Science and Technology, Otto Nielsens veg 10, Trondheim, 7052, Norway
[d] Department of Pipelines, Risers and Umbilicals, SINTEF Ocean, Otto Nielsens veg 10, Trondheim, 7052, Norway
[e] State Key Laboratory of Structural Analysis for Industrial Equipment, School of Ocean Science and Technology, Dalian University of Technology, No. 2 Dagong Road, Panjin, 124221, China

ARTICLE INFO

Keywords:
Dynamic power cable
Copper conductor
Bending behavior
Hysteresis effect
BFLEX

ABSTRACT

Reciprocating bending behavior is the main factor leading to the fatigue failure of dynamic power cables. However, in the research on the reciprocating bending behavior of dynamic cables, only the mechanical properties of the armored steel wire has been considered thus far and the copper conductor is disregarded. In this paper, the nonlinear bending properties of multilayer helically wound copper conductors are studied by experiments and numerical simulation. The research can provide accurate data of nonlinear bending mechanical properties of copper conductor for hydrodynamic analysis of dynamic cable fatigue life. Firstly, the nonlinear bending hysteresis curves of copper conductors are obtained by a reciprocating bending experiment of copper conductor. Secondly three-dimensional finite element numerical simulations of the copper conductor's bending behavior were also conducted. The numerical results from the finite element model were compared with the experimental data. Finally, sensitivity analysis of the structural parameters of the copper conductor was performed. The research shows that copper conductor has obvious nonlinear bending hysteresis behavior. The change of friction coefficient and radial extrusion pressure from the conductor's outer sheath layer have obvious effects on the critical sliding curvature and bending hysteresis properties of nonlinear bending properties of copper conductors.

1. Introduction

Dynamic power cables are key components in the development of marine resources and energy, such as offshore oil, gas and wind energies. To meet the structural requirements imposed by the marine environment, the dynamic power cable structure is designed for bending flexibility combined with sufficient axial and torsional resistance. Therefore, an unbonded multilayer helically wound structure is applied to meet the requirements, its typical cross-sectional form is shown in Fig. 1. This is also the case for conductor components, which is formed by winding a bunch of copper wires according to a specified laying angle of each layer, as shown in Fig. 2. Contact, slip and substantial friction between each individual wire in the same layer and among different layers of the conductor are the distinctive features of this structure. These structural features make the bending behavior of the whole structure to have nonlinear characteristics (Sævik and Ekeberg, 2002), which then affect the structural behavior of the product during storage, transportation, installation and operation.

Fatigue failure is an important failure mode of dynamic power cables in a marine dynamic environment (ISO 13628-5, 2009). Due to the load from waves and currents, the dynamic power cable structure undergoes reciprocating bending motion, and periodic sliding and friction will occur between the layers of the cable structure, often resulting in fatigue failure. The main components of dynamic power cables include copper conductor, steel armor wire, sheaths and fillers. The fatigue life prediction of dynamic power cables mainly considers the nonlinear mechanical properties of the steel armor wire the nonlinear bending behavior caused by the steel armor, but often omitting the nonlinear mechanical properties of copper conductors mainly due to its structure complexities (Sobhaniasl et al., 2020). With the increasing demand for power transmission by dynamic power cable, the volume

* Correspondence to: State Key Laboratory of Structural Analysis for Industrial Equipment, Department of Engineering Mechanics, Dalian University of Technology, No. 2 Linggong Road, Dalian, 116023, China.
E-mail address: yanjun@dlut.edu.cn (J. Yan).

https://doi.org/10.1016/j.oceaneng.2022.110831
Received 30 October 2021; Received in revised form 2 February 2022; Accepted 11 February 2022

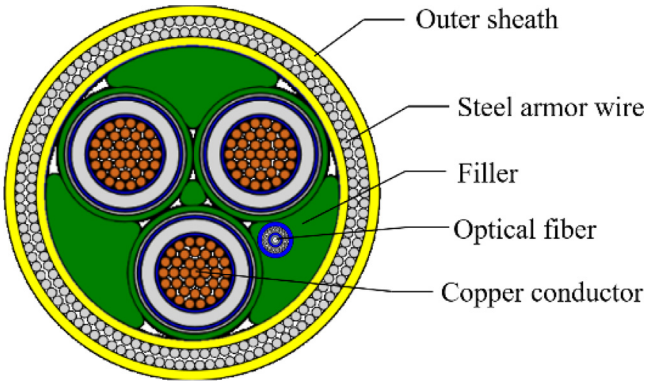

Fig. 1. A typical cross section of a dynamic power cable.

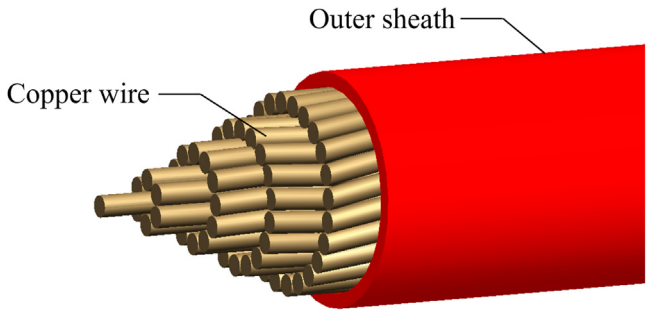

Fig. 2. Illustration of a typical multilayer helically wound copper conductor.

proportion of copper conductors in the cross section of dynamic power cables is increasing. Therefore, it is necessary to consider the nonlinear bending hysteresis behavior of the copper conductors and obtain accurate bending hysteresis curves in order to accurately calculate the fatigue life of dynamic power cables, which then can be used as inputs to global analysis and the prediction of the dynamic power cable fatigue life.

The nonlinear bending performance of the helically wound structure can be described by observing the relation of the bending moment and curvature as shown in Fig. 3. The curve is usually characterized by three stages (Lu et al., 2013): the OA segment is a stick zone, the AB segment is a slip transition zone, and the BC segment is a full slip zone. The curvature corresponding to point A is the initial sliding curvature κ_0, and the curvature corresponding to point B is the full sliding curvature κ_f. In engineering applications, the curvature corresponding to the tangent intersection of the OA segment and the BC segment, that is, point D, is usually called the critical slip curvature κ_{cr}. When the helically wound structure is further bent by reducing curvature after the point C, the bending moment and curvature relation is divided into another three stages as follows: the CA′ segment is a reverse stick zone, the A′B′ segment is a reverse slip transition zone, and the B′C′ segment is a reverse full slip zone. Among them, the curvature corresponding to point A′ is the reverse initial sliding curvature κ_0', and the curvature corresponding to point B′ is the reverse full sliding curvature κ_f'. The curvature corresponding to the tangent intersection of the CA′ segment and the B′C′ segment, that is, point D′, is defined as the reverse critical slip curvature κ_{cr}'.

Bending performance of helically wound structures such as umbilical cables, flexible pipes and marine cables has been well investigated by other researchers. Witz and Tan (1992) assumed that the structure only slides in the axial direction and obtained the bending stiffness calculation formula of the stick zone and the full slip zone. Ramos and Pesce (2004) established an analytical model for the bending stiffness of a helically wound structure based on the assumption of axial sliding. Due to ignoring the contact friction between layers, the bending moment in the analytical expression shows a linear change with curvature, which cannot accurately describe the nonlinear bending behavior of the helically wound structure. Fe'ret and Bournazel (1987) proposed another sliding hypothesis, believing that with bending deformation, the spiral should slide along the shortest path; that is, in addition to sliding along the axial direction, lateral sliding should also be considered, thereby obtaining the change in spiral curvature and then obtaining the stress distribution and sliding displacement of the spiral. Kraincanic and Kebadze (2001) proposed an analytical model without considering the friction nonlinear effect to simulate the bending process of the multilayer helically wound structure. In this paper, the change of the contact pressure due to the bending of the structure itself is ignored, and dynamic friction coefficient and static friction coefficient are equal. These researchers discovered that as the curvature increases, the layers will slide from completely nonsliding to partially sliding and then to fully sliding, presenting a state of nonlinear change. Zhang et al. (2008) verified the nonlinear and bending hysteresis effects of an unbonded helically wound structure through an experimental test. The above theoretical and experimental studies on the bending performance of the helically wound structure show that its bending stiffness presents nonlinear characteristics, however, most of these studies considered only the contact between layers while the contact within the same layer is barely taken into account and such interlayer contact is expected to be critical for a helically wound power cable.

Sævik (1993), based on the curved beam element, established a finite element formulation with kinematic couplings to study the bending stress and deformation of a single spiral steel wire. Probyn et al. (2007) and Le Corre and Probyn (2009) used the explicit analysis of the ABAQUS software to carry out three-dimensional finite element analysis of a multilayer helically wound structure. Shell and solid elements were used in the model, and a large number of surface-to-surface and line-to-surface contacts were considered. Therefore, the computational efficiency of the finite element model was relatively low. McNamara and Harte (1992) established a finite element model of a multilayer helically wound structure composed of isotropic layers and orthotropic layers but did not consider interlayer contact and friction. Jiang et al. (2013) proposed a three-dimensional model of an unbonded helically wound structure, considering nonlinear factors such as friction and contact. The numerical analysis results of the tensile, torsional and bending stiffness were obtained and compared with the test results in the literature. Zhang et al. (2015) conducted theoretical and numerical research on the bending characteristics of the helically wound structures and established a finite element model to compare with the experimental results. Lu et al. (2017) conducted a detailed study on the bending stress of multilayer helically wound structures. Based on theoretical models and numerical simulation methods, these scholars focused on the bending stress during the nonlinear bending process of helically wound structures. Li et al. (2019) and Li and Vaz (2020) studied the lateral instability mechanism of multilayer structures under cyclic bending and longitudinal compression loads through simulation and experiments and established an effective model that can describe the sliding process of such structures in the bending process, providing an analysis method for studying the lateral instability. Some scholars (Skeie et al., 2012; Ruan et al., 2017) have also carried out research studies on the reciprocating bending hysteretic phenomenon of the helically wound structures, but in these studies, only the linear mechanical properties of stick zone and full slip zone in the bending hysteretic phenomenon of structures were considered.

From the results of the above references review, it can be seen that both the theoretical analysis and finite element simulation of marine cable structures have been widely carried out, however, experimental investigations on the reciprocating bending behavior of the unbonded helically wound power cable are relatively limited. In addition, most of the above references only focused on the mechanical behavior of a single-layer unbonded helically wound structure in stick zone and full

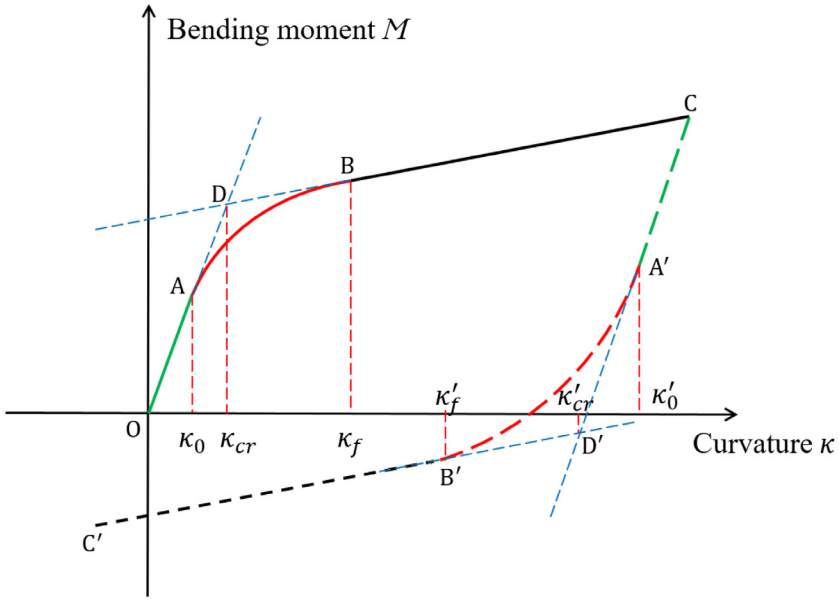

Fig. 3. Nonlinear bending behavior of a helically wound structure.

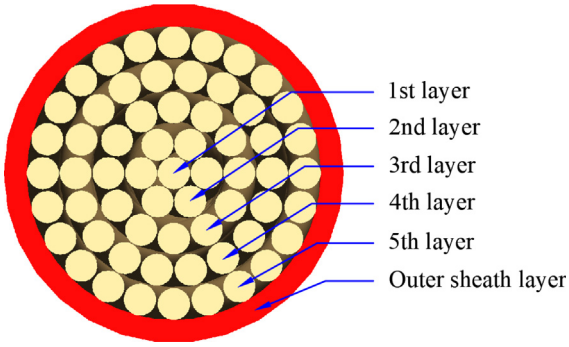

Fig. 4. A multilayer helically wound cross section of a copper conductor.

Table 1
Dimensions of the multilayer structure of the copper conductors.

Category	Value
The diameter of a single copper wire	2.35 mm
Number of copper wires in the first layer/winding angle (°)	1/0
Number of copper wires in the second layer/winding angle (°)	6/+3.7
Number of copper wires in the third layer/winding angle (°)	12/−7.4
Number of copper wires in the fourth layer/winding angle (°)	18/+11.2
Number of copper wires in the fifth layer /winding angle (°)	24/−15.0
The thickness of the outer sheath layer	1.5 mm

slip zone, while few references addressed on the reciprocating bending behavior of the copper conductors in the dynamic power cable. The conductor itself is a multilayer helically wound structure. In addition, in order to accurately predict the fatigue life of dynamic power cables, it is not enough to consider only the bending performance caused by the steel armor wires in cables, it is also necessary to study the nonlinear bending hysteretic behavior caused by the conductors in order to obtain accurate bending behavior of dynamic power cables. Few studies on the bending hysteresis of the copper conductors can be found. Therefore, to study the nonlinear bending behavior of dynamic power cables and predict their fatigue life more accurately, it is necessary to perform experimental research on the reciprocating bending behavior of the copper conductors.

Fig. 4 shows a typical cross section of multilayer copper conductor components in a dynamic power cable.

The main purpose of this paper is to study the nonlinear bending behavior of multi-layer helically wound copper conductors and obtain accurate nonlinear bending behavior of copper conductors. Accurate nonlinear bending performance curves of copper conductors can be used in the analysis of local stresses in dynamic cable fatigue life calculations. At the same time, the influence of key parameters of copper conductor on the bending nonlinear performance of copper conductor is studied, which can provide guidance for the processing and manufacturing of dynamic power cable.

The main research work in this paper is as follows: (1) The nonlinear bending behavior characteristics of this copper conductor are obtained through reciprocating bending experiments. (2) To study the influence of structural parameters on the bending behavior of the copper conductor, this paper considers nonlinear factors including interlayer friction and slip and establishes an accurate three-dimensional finite element model of the conductor component using BFLEX (Sævik, 2010), a special purpose finite element software for advanced structural analysis of flexible pipes and cables. The accuracy of the three-dimensional finite element simulation model is verified by comparing the numerical simulation results with the experimental results. (3) By changing the key structural parameters in the numerical model of the copper conductors, sensitivity studies of some structural parameters are carried out, focusing on the influence of the radial extrusion pressure of the outer sheath layer caused by different friction coefficients between layers and different fabrication processing technologies on the bending performance of the structure.

2. Experimental study

2.1. Bending test of the copper conductor

Referring to the international test specifications (ISO 13628-5, 2009; API 17B, 2014), this section presents a reciprocating bending experimental study on the copper conductor structure, as described in Table 1. The copper conductor consists of five-layers of the helically wound circular copper wires including one center wire and an outer sheath layer as a protective layer. The cross section of the copper conductor is shown in Fig. 4. Detailed structural dimensions are shown in Table 1.

The experiment was carried out in the laboratory of the School of Marine Science and Technology, Dalian University of Technology. As

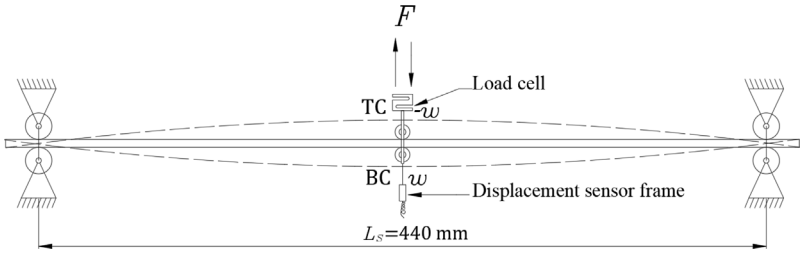

Fig. 5. Set-up of the reciprocating bending experiment of the copper conductor (F is the middle point reaction force; L_s is the copper conductor length between two hinge points; and w is the applied displacement of the copper conductor at the middle point).

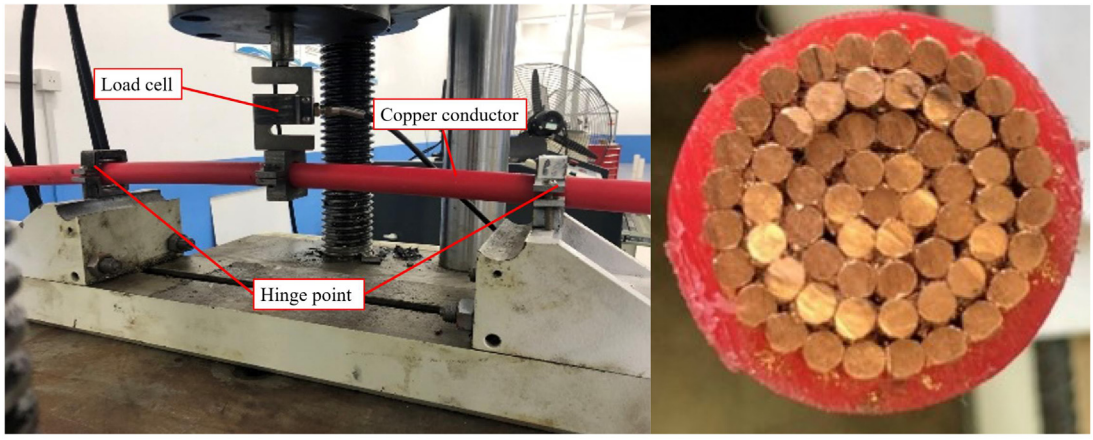

Fig. 6. Physical diagram of experimental conditions. (a) experimental equipments (b) cross-section of the copper conductor.

shown in Fig. 5, both ends of the copper conductor were restrained by hinge supports, and the middle point of the copper conductor was subjected to a vertical load, which can impose a reciprocating movement to the middle point of the copper conductor. The length of the test piece between the two hinged supports was 440 mm, which conforms to the recommended test length of the specification (ISO 13628-5, 2009; API 17B, 2014). The middle point of the copper conductor moves reversely at point C, as shown in Fig. 3, defining the upper load reverse point shown in Fig. 5 as the TC point and the lower load reverse point as the BC point. Displacement control was adopted in the loading program, and the displacement w and reaction force F applied in the copper conductor span are measured by the displacement sensor frame and the load cell. The upper and lower amplitude of displacement loading was 6 mm, and the loading rate was 0.2 mm·s^{-1}. The test process and the cross-section of the copper conductor are shown in Fig. 6.

To eliminate the influence of the initial bending curvature of the copper conductor on the experimental results, three reciprocating bending tests were carried out. In each test, three reciprocating displacement loads were applied at the middle point of the copper conductor, and data were collected after the load was stable. The test result of the third reciprocating load was used as the result representing the corresponding reciprocating bending test. After completing a reciprocating bending test, the reciprocating bending test was repeated after the cross section of the copper conductor was rotated 120 degrees, as shown in Fig. 7. Then, the average value of the three reciprocating bending test results was taken as the final experimental result of the reciprocating bending experiment of the copper conductor structure. According to the middle point displacement and the measured reaction force applied in the reciprocating bending experiment of the copper conductor structure, the middle point bending moment and curvature of the copper conductor structure can be obtained through formulas (1) and (2):

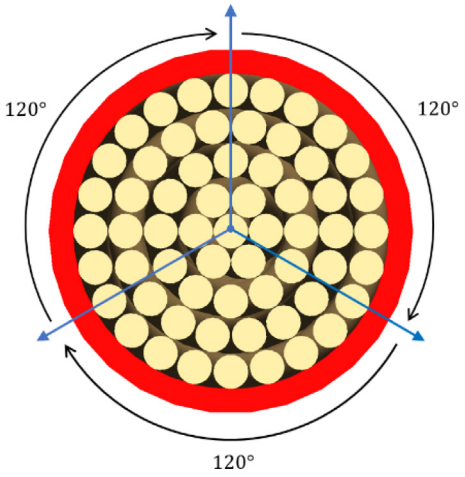

Fig. 7. Schematic diagram of copper conductor cross section rotated 120 degrees.

The formula for calculating the bending moment is:

$$M = \frac{FL_s}{4} \tag{1}$$

The curvature calculation formula is:

$$\frac{1}{\rho} = \frac{12w}{L_s^2} \tag{2}$$

Where $\frac{1}{\rho}$ is the curvature; F is the middle point reaction; L_s is the copper conductor length between two hinge points; w is the applied displacement of the copper conductor at the middle point; and M is the bending moment.

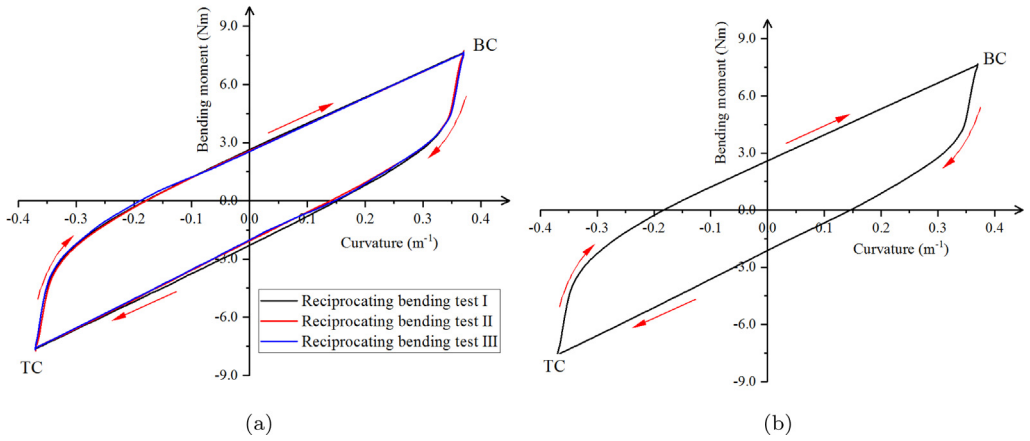

Fig. 8. Test results of the bending hysteretic curve of the cable conductor.(a) Three reciprocating bending test results (b) The average value of the three reciprocating bending test results.

2.2. Test results

The test data are plotted to obtain the reciprocating bending hysteretic curve of the copper conductor, as shown in Fig. 8(a). The loading sequence in the figure is TC-BC-TC in the clockwise direction (indicated by the red arrow).

From the experimental results, it can be seen that a hysteretic curve is formed in the reciprocating bending process of the copper conductor. When the bending stiffness of the copper conductor is loaded from the TC position to the BC position and reversed from the BC position to the TC position, the bending stiffness of the copper conductor gradually decreases and finally approaches a constant value, and the whole process presents the characteristics of a nonlinear change. From the intersection of the hysteresis curve and curvature coordinate axis, the mechanical behavior of the copper conductor structure under forward loading and reverse loading is not exactly the same. The reason for this phenomenon is that the vertical loading method is adopted in this experiment. During the experiment, when the copper conductor structure changes the loading direction at the bottom BC position and the top TC position, it is continuously subjected to gravity loading, which causes the bending moment of the slip transition zone to decrease at different speeds with curvature changes. By processing the TC to BC curve and the BC to TC curve data in Fig. 8(b), the curve of the bending experiment results shown in Fig. 8(b) can be fitted to obtain its slope at different positions, that is, the change of the bending stiffness of the copper conductor in the reciprocating bending process. The result is shown in Fig. 9.

From Fig. 9, when the reciprocating bending behavior of the copper conductor occurs, the bending stiffness of the overall structure presents nonlinear characteristics, and when the bending is reversed (shown at point a in Fig. 9), the maximum bending stiffness is 196.5 N m^2. When the bending curvature is small (shown at point b in Fig. 9), the overall bending stiffness of the copper conductor tends to a fixed value, and the average bending stiffness of the two curves (TC-BC segment and BC-TC segment) at the horizontal position is 14.4 N m^2. The results in Fig. 9 show that there is no three-stage bending stiffness nonlinearity, as described in Witz and Tan (1992). The reason is that the contact forces between the copper wires and between the copper wires and sheath layer is relatively small. Since the contact form between the copper wires is line-to-line contact or point-to-point contact, when the copper conductor undergoes relatively small curvature deformation, slippage occurs between the copper wires. The result measured at the beginning of this experiment is the result of the slip transition zone of the copper conductor bending hysteresis curve (that is, the hysteresis curve starts from the AB segment in Fig. 3), not the result of the stick zone (that is, the OA segment in Fig. 3 is very small in this example and has not been tested). This can be explained by noticing that the armored steel wires studied by Witz and Tan (1992) is helically wound at larger angles, and the rectangular cross section also makes the surface-to-surface contact more dominant. Therefore, when the armored steel wires exert larger contact force between layers, the armored steel wires will not slip easily, so there is a clear stick zone in the corresponding bending behavior.

From the TC-BC segment curve in Fig. 9, during the loading process with the loading curvature from −0.37 m^{-1} to 0.37 m^{-1}, the bending stiffness of the copper conductor stabilizes at −0.12 m^{-1}. When the curvature is −0.37 m^{-1} to −0.12 m^{-1}, the bending stiffness of the copper conductor is in the nonlinear change stage (the copper wires in the copper conductor are partially sliding). This stage in the figure accounts for approximately 33.78% of the entire process from TC to BC. This phenomenon shows that the nonlinear bending stage governs a large portion of the bending performance of the conductor. As the hysteresis effect will influence the global behavior of a dynamic riser in terms of damping, it is important to describe this phenomenon correctly for all cross-section components, including the conductors.

3. Finite element simulation

Due to the influence of nonlinear factors such as contact and friction in the reciprocating bending process of the copper conductor structure, accurate simulations are difficult via analytical formulas, so this section adopts the three-dimensional finite element method to simulate and verify the accuracy of the numerical model by comparing with the experimental results in the previous section. Furthermore, on the basis of numerical model validity, a sensitivity analysis of copper conductor structural parameters for the mechanical properties of the copper conductor structure is carried out. BFLEX (Sævik, 2010) software is a special purpose finite element analysis software for submarine flexibles and cables. This software can be used to carry out efficient finite element analysis on the cable structure considering the contact and friction effects between components. In this section, BFLEX is used to establish a three-dimensional finite element model of the copper conductor. By applying boundary constraints and middle point loads, the reciprocating bending behavior of the copper conductor structure can be simulated. According to formulas (1) and (2), the bending hysteretic curve of the copper conductor is calculated.

The three-dimensional finite element model of the copper conductor is shown in Fig. 10. The model length was 440 mm, and the diameter and helically wound angle of each layer of copper wire are listed in Table 1. The material parameters of copper wire, outer sheath layer and auxiliary layer are listed in Table 2. To facilitate the setting of

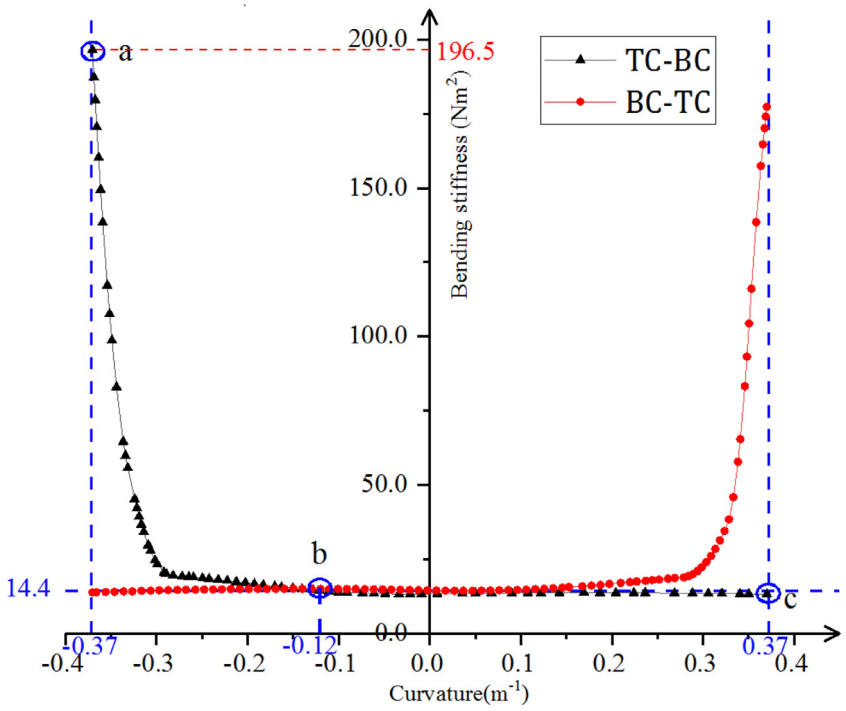

Fig. 9. Relation of the bending stiffness and curvature of the copper conductor.

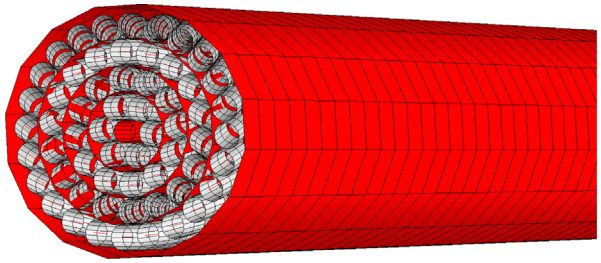

Fig. 10. Three-dimensional finite element model of the copper conductor by BFLEX.

the contact friction between the spirally wound copper wires, an auxiliary layer was defined between the layers for modeling convenience, ensuring smooth contact surfaces, for the benefit of computational performance. In the above finite element model, the HSHEAR353 element was used for the copper wires, and the HSHEAR363 element was used for the artificial layers and sheath layer (Sævik, 2010; Dai et al., 2017, 2018). HSHEAR353 is a beam element considering transverse and longitudinal slip, and HSHEAR363 is a combined beam and shell element that approximately describes local radial motion between layers. In the three-dimensional finite element model, HCONT454 and HCONT463 contact elements were used for contact friction. HCONT454 is a 4-node contact element developed for the circumferential contact friction between wires in the same helically wound layer. HCONT463 is a 3-node contact element developed for the radial contact friction of interlayer spirally wound wires.

In BFLEX, the radial extrusion pressure of the outer sheath layer on the copper conductor can be obtained by applying axial initial strain to the outer sheath layer. By applying axial initial strain to the outer sheath layer of the copper conductor, the radial extrusion pressure of the outer sheath layer on the copper conductor can be obtained by the following Eq. (3). Eq. (3) can be obtained by simplifying Lamé equation (Lamé, 1859).

$$p = \frac{2E\epsilon t}{\pi d \upsilon} \tag{3}$$

Table 2
Material parameters.

	Poisson's ratio	Young's modulus (Pa)
Copper wire	0.30	1.18e11
Outer sheath layer and auxiliary layer	0.35	4.20e8

where p is the radial extrusion pressure; E is the Young's modulus; ϵ is the axial initial strain; t is the thickness of outer sheath layer; d is the inner diameter of outer sheath layer; and υ is the Poisson's ratio.

According to Dai et al. (2017) and Nasution et al. (2014), the coefficient of friction among the copper wires was set to 0.2, whereas the coefficient of friction between the sheath layer and the copper conductors was set to 0.3. An axial initial strain of 0.01 was applied to the outer sheath layer, that is, the radial extrusion pressure was 0.542 MPa. After the numerical simulation calculation of BFLEX software, the stress diagram of each layer of the copper conductor at the BC position is shown in Fig. 11. The maximum stress of each layer occurs in the middle of each layer. The maximum stress of the 1st layer is 31.5 MPa; the maximum stress of the 2nd layer is 51.2 MPa; the maximum stress of the 3rd layer is 52.9 MPa; the maximum stress of the 4th layer is 54.7 MPa; the maximum stress of the 5th layer is 56.6 MPa; the maximum stress of the outer sheath layer is 6.7 MPa. The maximum value of structural stress is in the 5th layer. Results for the BFLEX simulation are compared with the experimental test results, as shown in Fig. 12.

Fig. 12 shows that the three-dimensional finite element simulation using BFLEX is in good agreement with the nonlinear bending hysteresis curve of the copper conductor obtained from the experiment. At the same time, the bending stiffness of the slip transition zone from the BC point to the TC point, the critical curvature of the transition from the slip transition zone to the full slip zone, and other characteristic points also have good accuracy. There is a certain mismatch in the reverse bending stage from the TC point to the BC point. The main reason for this mismatch is that the dynamic copper conductor is longer at the outer ends of the two hinge supports in the experiment, and the gravity at the end of the copper conductor causes the copper conductor to bend upward in the middle of the span. That is, when the bending

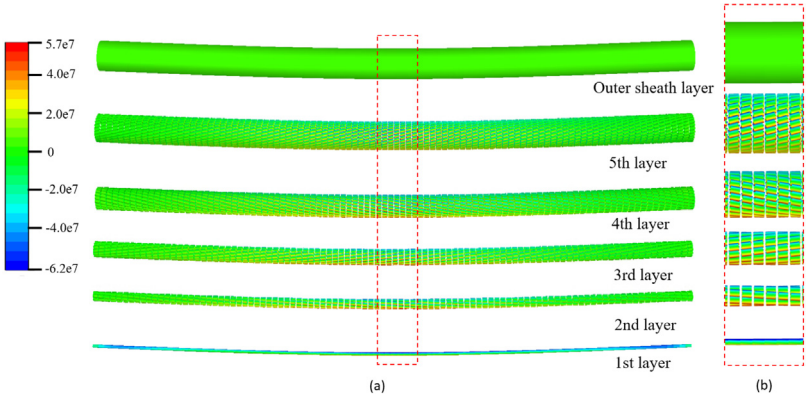

Fig. 11. Structural stress diagram of each layer of copper conductor at BC position. (a) Overall structural stress diagram of each layer (b) Partially enlarged stress diagram in the middle of each layer.

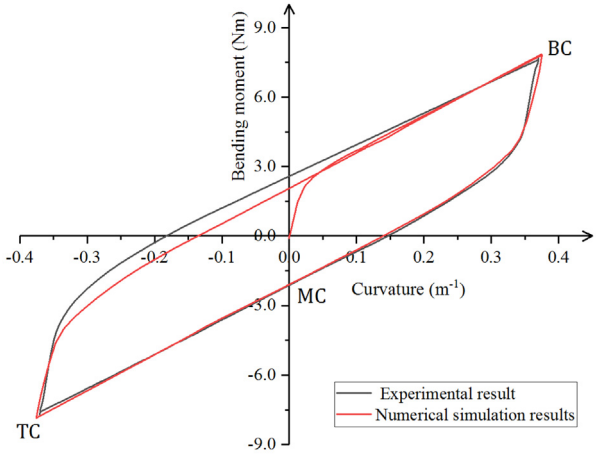

Fig. 12. Comparison of the experimental and numerical simulation results of the copper conductor.

moment is zero from point TC to point BC in Fig. 12, the absolute value of the curvature of the copper conductor at this time is greater than the numerical simulation result. However, it is difficult for the finite element model in BFLEX to capture the influence of the above factors.

The bending stiffness (in the current engineering practice, the fatigue analysis of dynamic power cables usually adopts the bending stiffness of the cable structure in the full slip zone (Chen et al., 2016)) of the three-dimensional finite element numerical simulation results in the full slip zone (Segment MC to TC in Fig. 12) is 15.2 N m^2, compared with the experimental test result of 14.4 N m^2, and the difference is about 5.6%. When the copper conductor is subjected to reciprocating bending loads, energy loss will occur due to heat dissipation caused by friction. The envelope area of the bending hysteresis curve can well reflect this damping property of the copper conductor structure. The envelope area can be obtained by integrating the bending hysteresis curve of the experimental results and numerical simulation results shown in Fig. 12. The envelope area of the bending hysteresis curve from the experimental result is 3.185 N m m^{-1}, the envelope area of the bending hysteresis curve from the finite element simulation is 2.875 N m m^{-1}, and the difference between the two is 9.73%. Furthermore, the reverse critical slip curvature (κ'_{cr} in Fig. 3) is compared and analyzed according to the experimental and numerical simulation results. Through data fitting, the reverse critical slip curvature in the experimental test results is 0.3319 m^{-1}, while the reverse critical slip curvature in the numerical simulation results is 0.3431 m^{-1}, and the difference is only 3.26%. Hence, it can be concluded that the three-dimensional finite element model established by BFLEX can accurately simulate the reciprocating bending behavior of the copper conductor.

4. Sensitivity analysis

Due to the differences in material selection, manufacturing technology and installation and application environment of the copper conductors during manufacturing and service, the friction coefficient between the copper conductor interlayer materials may vary. Moreover, the outer sheath of the copper conductor generally adopts a hot extrusion molding process (Dan et al., 2015), there is a certain initial strain of inward shrinkage after the sheath layer is cooled down, and different manufacturing process may lead to different initial strains. The initial strain on the outer sheath layer will produce radial extrusion pressure on the conductor, and then affect the contact friction among copper wires in the conductor. Therefore, it is necessary to study the influence of the friction coefficient and radial extrusion pressure of the sheath layer on the structural bending hysteretic effect. In this section, the sensitivity analysis of key structural parameters of the copper conductor was carried out by using the three-dimensional finite element model established in the previous section.

4.1. Sensitivity analysis of the friction coefficients

There are two main types of materials in the copper conductor, namely, copper wire metal material and sheath layer nonmetal material. Therefore, two friction coefficients in the copper conductor will be studied, i.e. the friction coefficient among the copper wires and the friction coefficient between the copper wire and sheath layer.

4.1.1. Sensitivity analysis of the friction coefficient between the copper wire and sheath layer

The friction coefficient between the copper wire and sheath layer of the copper conductor was set to different values in the analysis. According to the range of friction coefficients between the copper wire and sheath layer in the common copper conductor structure, the friction coefficient was divided into five groups, which were 0.1, 0.2, 0.3, 0.4, and 0.5, the axial initial strain of the outer sheath layer was set to 0.01, which corresponds to a radial extrusion pressure of 0.542 MPa. The friction coefficient among copper wires was set to 0.2. The simulation results are shown in Fig. 13.

As shown in Fig. 13, with increasing friction coefficient, the area of the bending hysteretic curve of copper conductor reciprocating bending increases continuously. This is because with the gradual increase in the friction coefficient, the energy loss caused by the friction effect in the process of the copper conductor bending up and down gradually increases. The envelope area of the curve can be obtained by integrating

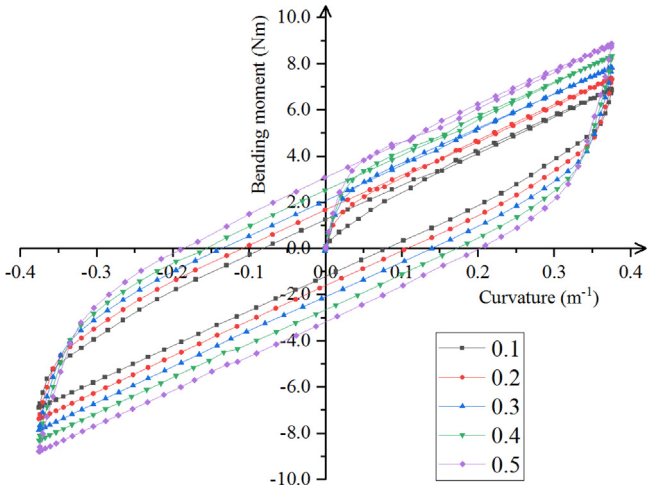

Fig. 13. Bending hysteresis curve of the copper conductor structure under different friction coefficients between the copper wire and sheath layer.

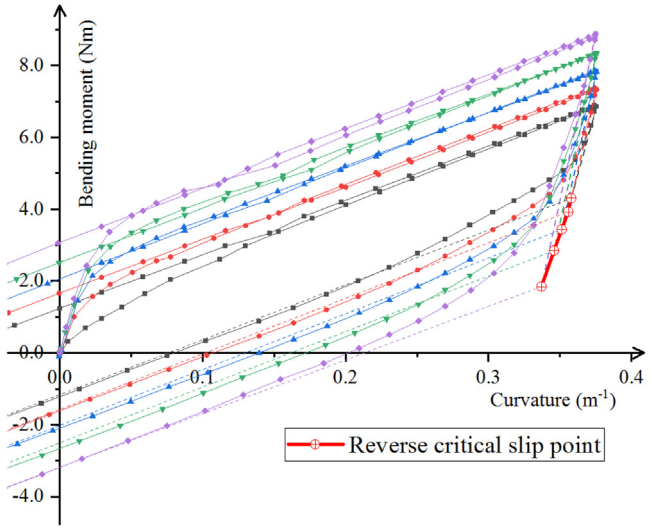

Fig. 14. Variation of the reverse critical slip point under different friction coefficients between the copper wire and the sheath layer.

Table 3
The influence of the friction coefficient between the copper wire and sheath layer on the envelope area and reverse critical slip curvature of the hysteresis curve.

Friction coefficient	0.1	0.2	0.3	0.4	0.5
Envelope area (N m m^{-1})	1.634	2.258	2.875	3.489	4.142
Reverse critical slip curvature (m^{-1})	0.3579	0.3558	0.3513	0.3459	0.3371

the bending hysteretic curves of the copper conductor structures under different friction coefficients. The reverse critical slip curvature (i.e., D′ point in Fig. 3) of each curve in Fig. 13 was calculated by processing the numerical results, as in Section 3. The results are shown in Fig. 14 and Table 3.

Fig. 14 is a partial enlargement of Fig. 13. The position coordinates of the reverse critical slip point are obtained by tangent intersection in Fig. 14. It can be seen from the figure that the reverse critical slip point is obviously affected by the change of friction coefficient between the copper wire and the sheath layer, and the position coordinate is linear distribution. From Table 3 and Fig. 15, the enveloping area of the hysteretic curve shows a linear growth trend with an increase in the friction coefficient between the copper wire and the sheath layer. The above phenomenon shows that with increasing friction coefficient,

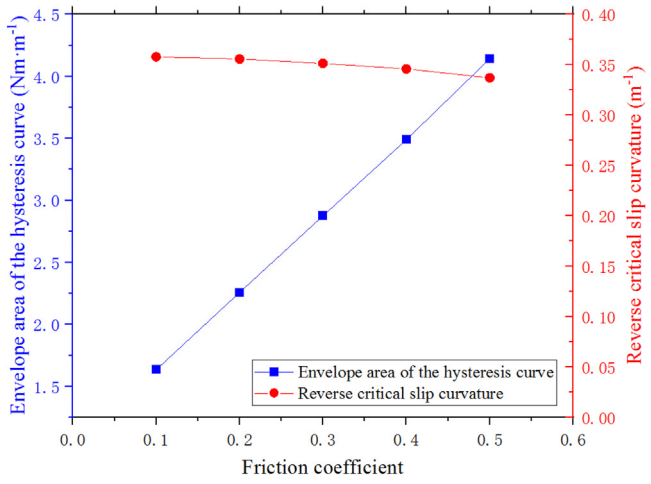

Fig. 15. Sensitivity analysis of the friction coefficient between the copper wire and sheath layer.

the energy loss caused by friction is linearly related to the friction coefficient between the copper wire and sheath layer in the reciprocating bending behavior. The reverse critical slip curvature has a nonlinear decreasing trend with increasing friction coefficient between the copper wire and the sheath layer. Therefore, when the friction coefficient increases and the copper conductor undergoes reverse bending, the required curvature of the copper conductor structure from non-sliding to critical sliding gradually increases. When the maximum bending curvature is 0.372 m^{-1}, the variation of the reverse critical slip curvature is very small, and the population variance of the reverse critical slip curvature is 5.6e−05 m^{-2} for different friction coefficients. The above phenomena show that the friction coefficient between the copper wire and the sheath layer has little influence on the reverse critical slip curvature of the copper conductor. The friction coefficient between the copper wire and the sheath layer has a more obvious influence on the reverse stick zone and the reverse slip transition zone. This effect can be clearly seen from Fig. 13. It can be observed that under the influence of different friction coefficients, the full slip zone of the curve is almost parallel under different friction coefficients, which shows that the friction coefficient between the copper wire and the sheath layer has very little effect on the bending performance of the structure when the structure is fully sliding.

4.1.2. Sensitivity analysis of the friction coefficient among copper wires

The friction coefficient among the copper wires of the copper conductor was set to different values in this analysis. According to the range of friction coefficients among copper wires in a common cable structure, the friction coefficient was divided into five groups, which were 0.1, 0.2, 0.3, 0.4, and 0.5. The axial initial strain of the outer sheath layer was set to 0.01, corresponding to a radial extrusion pressure of 0.542 MPa. The friction coefficient between the copper wire and sheath layers was set to 0.3. The simulation results are shown in Fig. 16.

From Fig. 16, with increasing friction coefficient among copper wires, the area of the copper conductor reciprocating bending hysteretic curve gradually increases, but the increase is very small, far lower than the increase ratio of the friction coefficient between the copper wire and sheath layer to the envelope area of the hysteretic curve in Fig. 13. This result shows that the energy loss caused by the friction effect among copper wires is not proportionally affected by the change of the friction coefficient among copper wires in the cyclic bending of the copper conductor. Integrating the bending hysteresis curve of copper conductors under different coefficients of friction among copper wires, the envelope area of the hysteresis curve can be obtained

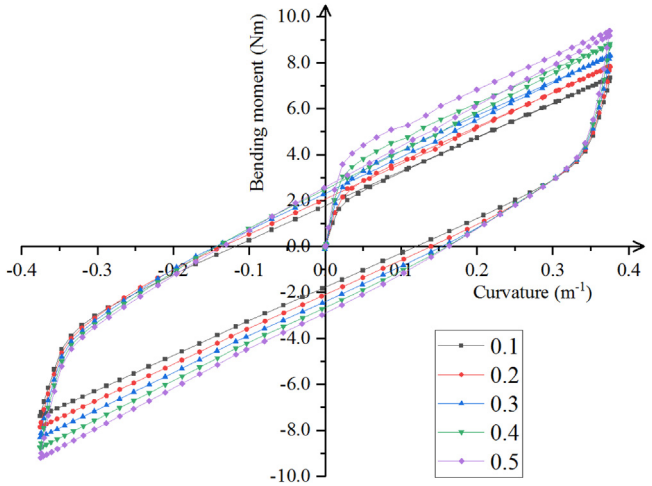

Fig. 16. Bending hysteresis curve of the copper conductor structure under different friction coefficients among copper wires.

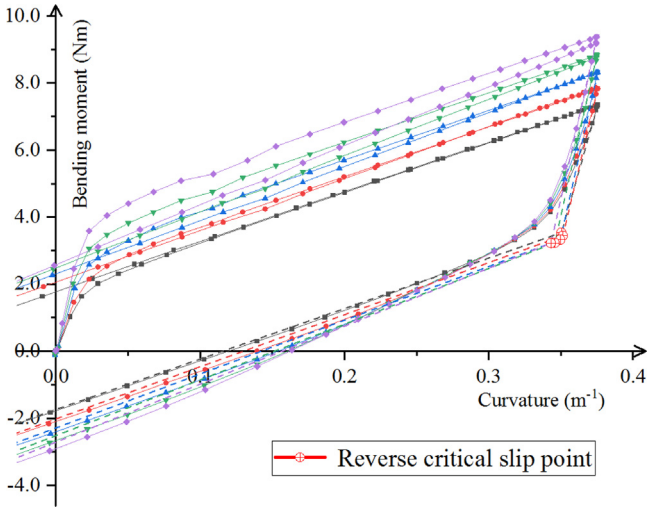

Fig. 17. Variation of the reverse critical slip point under different friction coefficients among the copper wires.

Table 4
The influence of the friction coefficient among the copper wires on the envelope area and reverse critical slip curvature of the hysteresis curve.

Friction coefficient	0.1	0.2	0.3	0.4	0.5
Envelope area (N m m^{-1})	2.470	2.875	3.197	3.453	3.655
Reverse critical slip curvature (m^{-1})	0.3503	0.3513	0.3496	0.3457	0.3431

quantitatively. At the same time, the reverse critical slip curvature (i.e., D′ point in Fig. 3) of each curve in Fig. 16 was calculated by processing the results as in Section 3. The results are shown in Fig. 17 and Table 4.

Fig. 17 is a partial enlargement of Fig. 16. At the same time, the position coordinates of the reverse critical slip point are obtained by tangent intersection in Fig. 17. It can be seen that the reverse critical slip point is little affected by the change of friction coefficient among the copper wires, and is almost at the same position. From Table 4 and Fig. 18, the enveloping area of the hysteretic curve shows a nonlinear growth trend with increasing friction coefficient among copper wires, and the growth ratio gradually decreases. The above phenomenon shows that with increasing friction coefficient among the copper wires, the influence of the friction coefficient on the energy loss caused by friction gradually decreases in the reciprocating bending

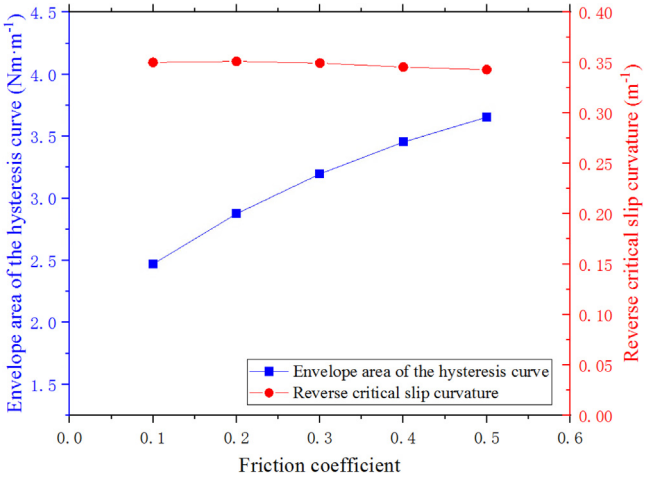

Fig. 18. Sensitivity analysis of the friction coefficient among copper wires and the bending hysteretic curve.

behavior. When the maximum bending curvature is 0.372 m^{-1}, the variation of the reverse critical slip curvature is very small, and the population variance of the reverse critical slip curvature is 4.5e−06 m^{-2} under different friction coefficients. The above phenomena show that the critical slip curvature is hardly affected by the friction coefficient among the copper wires. It can be observed that when the structure is fully sliding, with increasing friction coefficient, the slope of the full slip zone of the curve presents an obvious increasing trend, which shows that the friction coefficient among copper wires has an obvious influence on the bending stiffness of the structure when the structure is fully sliding.

From the comparison of Figs. 15 and 18, under the same coordinate axis, the influence of the friction coefficient between the copper wire and the sheath layer on the envelope area of the hysteretic curve and the reverse critical slip curvature is greater than that among the copper wires. Therefore, the influence of the friction coefficient between the sheath layer and the copper wire on the bending performance of the copper conductor structure should be taken into account in engineering applications.

4.2. Sensitivity analysis of the radial extrusion pressure of the outer sheath layer

To study the influence of the radial extrusion pressure of the outer sheath layer on the reciprocating bending behavior, the radial extrusion pressure cannot be directly applied to the outer sheath layer in the established three-dimensional finite element model for calculation. Therefore, in the software, the radial extrusion pressure was applied by applying the axial initial strain to the outer sheath layer. The axial initial strains were divided into five groups, which were 0.01, 0.02, 0.03, 0.04 and 0.05 respectively, and the corresponding radial extrusion pressures are 0.542 MPa, 1.084 MPa, 1.625 MPa, 2.167 MPa and 2.709 MPa respectively. The friction coefficient among the copper wires was set to 0.2, and the friction coefficient between the sheath layer and copper wires was set to 0.3.

Carrying out a three-dimensional finite element numerical simulation on the above groups, the calculation results of the bending hysteresis curve of the copper conductor structure can be obtained, as shown in Fig. 19.

Similar to the analysis in the previous section, this section also analyzes the influence of the radial extrusion pressure of the outer sheath layer on the envelope area of the hysteresis curve and the reverse critical slip curvature. Fig. 20 is a partial enlargement of Fig. 19. It can be seen from Fig. 20 that the reverse critical slip point exhibits

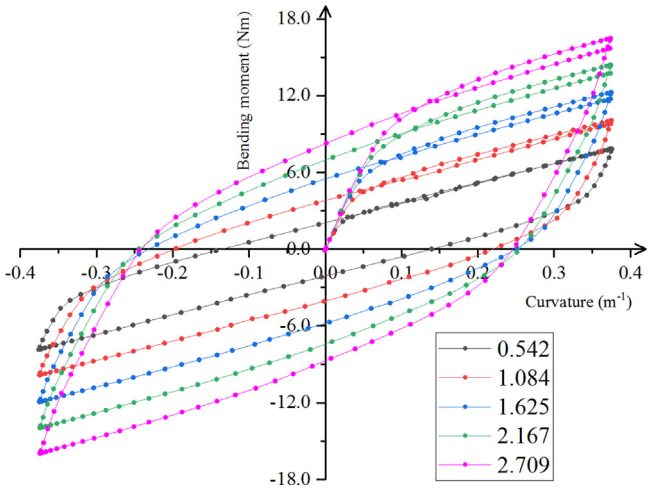

Fig. 19. Bending hysteresis curve of the copper conductor structure under different radial extrusion pressure of the outer sheath layer.

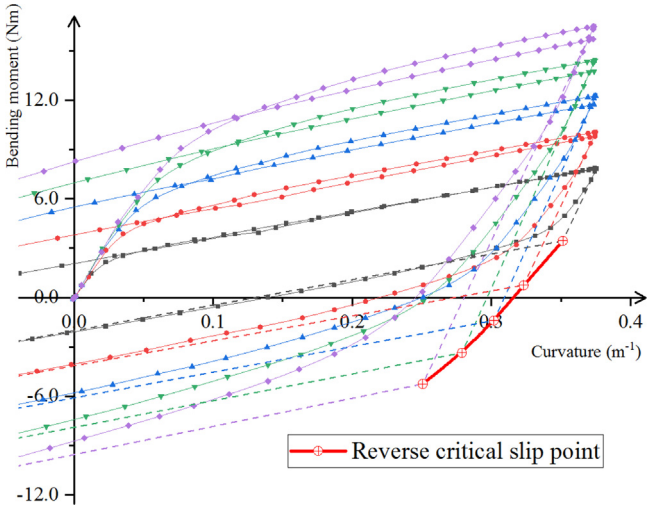

Fig. 20. Variation of the reverse critical slip point under different radial extrusion pressure of the outer sheath layer.

Table 5
Influence of the envelope area of the hysteretic curve with radial extrusion pressure.

Radial extrusion pressure (MPa)	0.542	1.084	1.625	2.167	2.709
Envelope area (N m m^{-1})	2.873	4.984	6.904	8.545	9.889
Reverse critical slip curvature (m^{-1})	0.3513	0.3232	0.3018	0.2788	0.2507

an obvious linear distribution with the increase of the radial extrusion pressure of the outer sheath layer. Table 5 shows the relationship between the envelope area of the hysteretic curve and the reverse critical slip curvature of the copper conductor structure corresponding to different radial extrusion pressures. In Fig. 21, the sensitivity analysis results of the radial extrusion pressure of the sheath layer to the envelope area of the hysteretic curve and the reverse critical slip curvature are further visually displayed through curves.

From Fig. 19, the radial extrusion pressure of the sheath layer has a great influence on the copper conductor bending hysteretic curve. The greater the radial extrusion pressure of the sheath layer is, the more energy the copper conductor consumes during the bending process. From the curve of Fig. 19, it can be observed that with an increase in the radial extrusion pressure value of the outer sheath layer, the curvature of the position where the curve overlaps during the initial bending and reciprocating bending of the copper conductor gradually

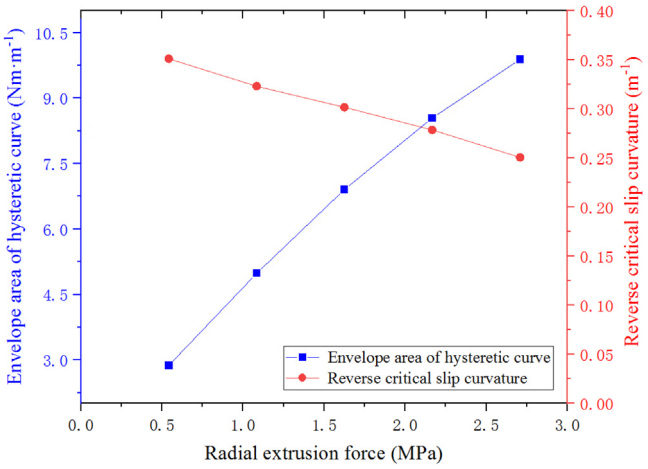

Fig. 21. Sensitivity analysis of the radial extrusion pressure of the sheath layer to the bending hysteretic curve.

increases. This phenomenon indicates that the total sliding curvature κ_f of the copper conductor structure gradually increases; that is, when the same bending curvature occurs, the proportion of the slip transition zone in the entire bending stage gradually increases. With the change in parameters, the importance of the slip transition zone is highlighted, which should be considered in engineering applications. From the data in Table 5 and Fig. 21, the envelope area of the hysteresis curve gradually increases with increasing radial extrusion pressure, indicating that an increase in external pressure increases the friction energy consumption among copper wires, making the damping performance of the copper conductor structure more significant. At the same time, from the analysis of the data growth trend, we can observe that this trend is characterized by a weak nonlinearity. With the increase in the radial extrusion pressure of the sheath layer, the value of reverse critical slip curvature decreases linearly, which means that the slip curvature increases linearly in reverse bending. Therefore, when the copper conductor undergoes reverse bending, the required curvature of the copper conductor structure from nonsliding to critical slip is gradually increased with the increases of the radial extrusion pressure of the sheath layer. When the maximum bending curvature is 0.372 m^{-1}, the variation of the reverse critical slip curvature has a large variation range, and the population variance of the reverse critical slip curvature is 1.2e−03 m^{-2} under different radial extrusion pressure of the sheath layer. The radial extrusion pressure of the sheath layer has an obvious influence on the reverse stick zone and the reverse slip transition zone.

5. Conclusion

In this paper, the reciprocating bending behavior of a multilayer copper conductor in a dynamic power cable was studied by both experimental and numerical studies. Sensitivity analysis on key structural parameters were carried out. The following conclusions can be drawn:

1. When the copper conductor structure is subjected to reciprocating bending, its bending performance presents obvious nonlinear characteristics. The finite element model was able to accurately simulate the bending behavior of the copper conductor.
2. From the results of experiment and numerical simulation, it can be seen that the non-linear bending performance of the copper conductor is mainly in the slip transition zone and the full slip zone, instead of in the stick zone, most probably due to the line-to-line contact or point-to-point contact among the copper wires.

3. Through sensitivity analysis of the parameters in the copper conductor numerical model, it can be seen that the friction coefficient has an obvious influence on the nonlinear bending performance of the copper conductor. The friction coefficient between the sheath layer and the copper wire mainly affects the slip transition zone in the nonlinear performance of the copper conductor. The friction coefficient among copper wires mainly affects the full slip zone in the nonlinear performance of the copper conductor.
4. The radial extrusion pressure of the outer sheath layer has obvious influence on bending nonlinearity of the copper conductor. It is therefore necessary not to neglect the influence of deep water pressure on bending performance of the copper conductor. In the fatigue life analysis of dynamic power cables consisting multilayer helically wound copper conductors, attention should be given to the nonlinear characteristics of bending performance and the influence of key structural parameters on bending performance should also be evaluated.

CRediT authorship contribution statement

Haitao Hu: Conceptualization, Methodology, Software, Writing – original draft, Formal analysis. **Jun Yan:** Conceptualization, Methodology, Supervision, Writing – review & editing. **Svein Sævik:** Conceptualization, Software, Writing – review & editing. **Naiquan Ye:** Methodology, Software, Writing – review & editing. **Qingzhen Lu:** Validation, Resources. **Yufeng Bu:** Investigation, Data curation.

Declaration of competing interest

The authors declare that they have no known competing financial interests or personal relationships that could have appeared to influence the work reported in this paper.

Acknowledgments

The authors highly appreciate the financial support provided by the National Natural Science Foundation of China (No. U1906233), the Key R&D Program of Shandong Province(2019JZZY010801), the Fundamental Research Funds for the Central Universities (DUT20ZD213, DUT20LAB308), the International Cooperation Training Program for Innovative Talents of Norwegian University of Science and Technology (NTNU) and China Scholarship Council (CSC).

References

API 17B, 2014. Recommended Practice for Flexible Pipe, Vol. 44, Third ed. American Petroleum Institute, Washington, DC.

Chen, J., Yan, J., Yue, Q., Tang, M., 2016. Flexible riser configuration design for extremely shallow water with surrogate-model- based optimization. J. Offshore Mech. Arct. Eng. (ISSN: 1528896X) 138 (4), 041701.

Dai, T., Sævik, S., Ye, N., 2017. Friction models for evaluating dynamic stresses in non-bonded flexible risers. Mar. Struct. 55 (sep.), 137–161.

Dai, T., SæVik, S., Ye, N., 2018. An anisotropic friction model in non-bonded flexible risers. Mar. Struct. 59 (may), 423–443.

Dan, D., Sun, L., Guo, Y., Cheng, W., 2015. Study on the mechanical properties of stay cable HDPE sheathing fatigue in dynamic bridge environments. Polymers (ISSN: 2073-4360) 7 (8), 1564–1576.

Fe'ret, J.J., Bournazel, C.L., 1987. Calculation of stresses and slip in structural layers of unbonded flexible pipes. (ISSN: 0892-7219) 109, 263–269.

ISO 13628-5, 2009. Petroleum and Natural Gas Industries - Design and Operation of Subsea Production Systems - Part 5: Subsea Umbilicals. English.

Jiang, H., Yang, H., Liu, H., 2013. Experimental and numerical analysis of a new simplified model for the deepwater unbonded flexible risers. Chin. J. Ship Res. 8 (1), 64–72.

Kraincanic, I., Kebadze, E., 2001. Slip initiation and progression in helical armouring layers of unbonded flexible pipes and its effect on pipe bending behaviour. J. Strain Anal. Eng. Des. (ISSN: 03093247) 36 (3), 265–275.

Lamé, G., 1859. LeÇOns sur Les CoordonnÉEs Curvilignes Et Leurs Diverses Applications. Mallet-Bachelier.

Le Corre, V., Probyn, I., 2009. Validation of a 3-dimensional finite element analysis model of a deep water steel tube umbilical in combined tension and cyclic bending. In: Proceedings of the International Conference on Offshore Mechanics and Arctic Engineering - OMAE, Vol. 3: Pipeline and Riser Technology. pp. 77–86.

Li, X., Vaz, M.A., 2020. Frictional effect on circular armour wire lateral buckling in umbilicals. Ocean Eng. 220 (9), 108306.

Li, X., Vaz, M.A., Custodio, A.B., 2019. Analytical and experimental studies on flexible pipes tensile armors lateral instability in cyclic bending. Mar. Struct. 67 (SEP.), 102630.

Lu, Q., Feng, L., Yan, J., 2013. Time domain analysis of flexible risers considering non-linear bending stiffness. J. Harbin Eng. Univ. (ISSN: 10067043) 34 (11), 1352–1356.

Lu, Q., Yang, Z., Yan, J., Lu, H., Chen, J., Yue, Q., 2017. A finite element model for prediction of the bending stress of umbilicals. J. Offshore Mech. Arct. Eng. (ISSN: 0892-7219) 139 (6), 061302.

McNamara, J.F., Harte, A.M., 1992. Three-dimensional analytical simulation of flexible pipe wall structure. J. Offshore Mech. Arct. Eng. (ISSN: 1528896X) 114 (2), 69–75.

Nasution, F.P., Sæ vik, S., Gjøsteen, J.K., 2014. Finite element analysis of the fatigue strength of copper power conductors exposed to tension and bending loads. Int. J. Fatigue (ISSN: 01421123) 59, 114–128.

Probyn, I., Dobson, A., Martinez, M., 2007. Advances in 3-D FEA techniques for metallic tube umbilicals. In: Proceedings of the International Offshore and Polar Engineering Conference. (ISSN: 10986189) ISOPE-I-07-334.

Ramos, R., Pesce, C.P., 2004. A consistent analytical model to predict the structural behavior of flexible risers subjected to combined loads. J. Offshore Mech. Arct. Eng. (ISSN: 08927219) 126 (2), 141–146.

Ruan, W., Bai, Y., Yuan, S., 2017. Dynamic analysis of unbonded flexible pipe with bend stiffener constraint and bending hysteretic behavior. Ocean Eng. (ISSN: 00298018) 130, 583–596.

Sævik, S., 1993. A finite element model for predicting stresses and slip in flexible pipe armouring tendons. Comput. Struct. (ISSN: 00457949) 46 (2), 219–230.

Sævik, 2010. Bflex Theory Manual. Marintek.

Sævik, S., Ekeberg, K.I., 2002. Non-linear stress analysis of complex umbilical cross-sections. In: Proceedings of the International Conference on Offshore Mechanics and Arctic Engineering - OMAE, vol. 1. pp. 211–217.

Skeie, G., Sødahl, N., Steinkjer, O., 2012. Efficient fatigue analysis of helix elements in umbilicals and flexible risers: Theory and applications. J. Appl. Math. (ISSN: 1110757X) 2012, 246812.

Sobhaniasl, M., Petrini, F., Karimirad, M., Bontempi, F., 2020. Fatigue life assessment for power cables in floating offshore wind turbines. Energies 13 (12), 3096.

Witz, J.A., Tan, Z., 1992. On the flexural structural behaviour of flexible pipes, umbilicals and marine cables. Mar. Struct. 5 (2–3), 205–227.

Zhang, M., Chen, X., Fu, S., Guo, Y., Ma, L., 2015. Theoretical and numerical analysis of bending behavior of unbonded flexible risers. Mar. Struct. (ISSN: 09518339) 44, 311–325.

Zhang, J., Tan, Z., Sheldrake, T., 2008. Effective bending stiffness of an unbonded flexible riser. In: Proceedings of the International Conference on Offshore Mechanics and Arctic Engineering - OMAE, Vol. 48203. pp. 117–123.